

SUPPLEMENTARY INFORMATION

SUPPLEMENTARY FIGURES

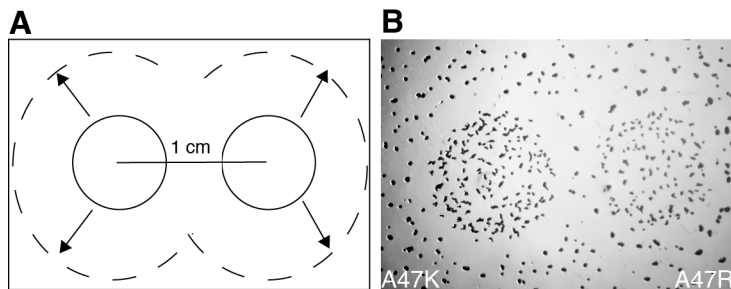


Figure S1. Colony-encounter assay. **A.** Initially separate colonies (solid circles) grow and swarm outward (arrows) and freely merge (as depicted here) in the absence of kin discrimination barriers. **B.** Self-self encounter control of oncoming colonies of the same natural isolate (A47) that differ only in their antibiotic-resistance marker. ‘K’ and ‘R’ indicate kanamycin- and rifampicin-resistance marked variants of A47, respectively. No interface demarcation line between colonies was visible for any self-self encounters. Dark spots are individual fruiting bodies.

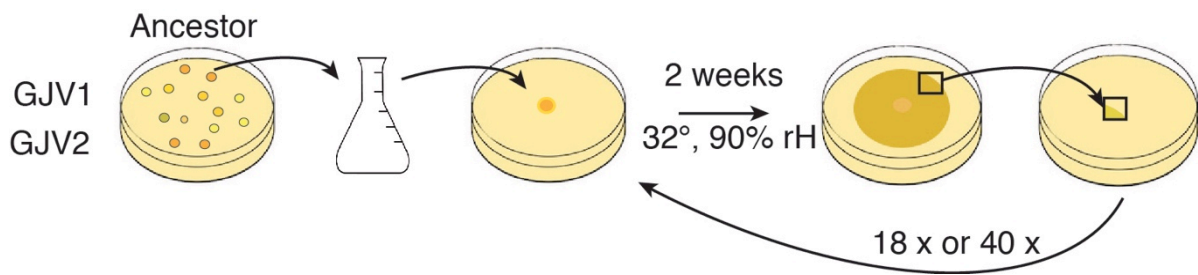


Figure S2. Experimental evolution. Independent clones from differentially marked ancestor variants (either rifampicin sensitive (GJV1) or resistant (GJV2)) were grown in liquid and used to start experimental evolution populations. A total of 104 independent populations were established across twelve different agar-plate environments (see Table S2). Each population was allowed to grow and swarm outward for two weeks at 32 °C and 90% rH. At two-week intervals, a small rectangle (~3 mm x 5 mm) was cut out from the point along the swarm perimeter furthest from the colony center (or from a random point if no deviation from circularity was evident) and placed upside-down on the center of a new plate. This process was repeated for either 18 or 40 cycles, depending on the environmental treatment.

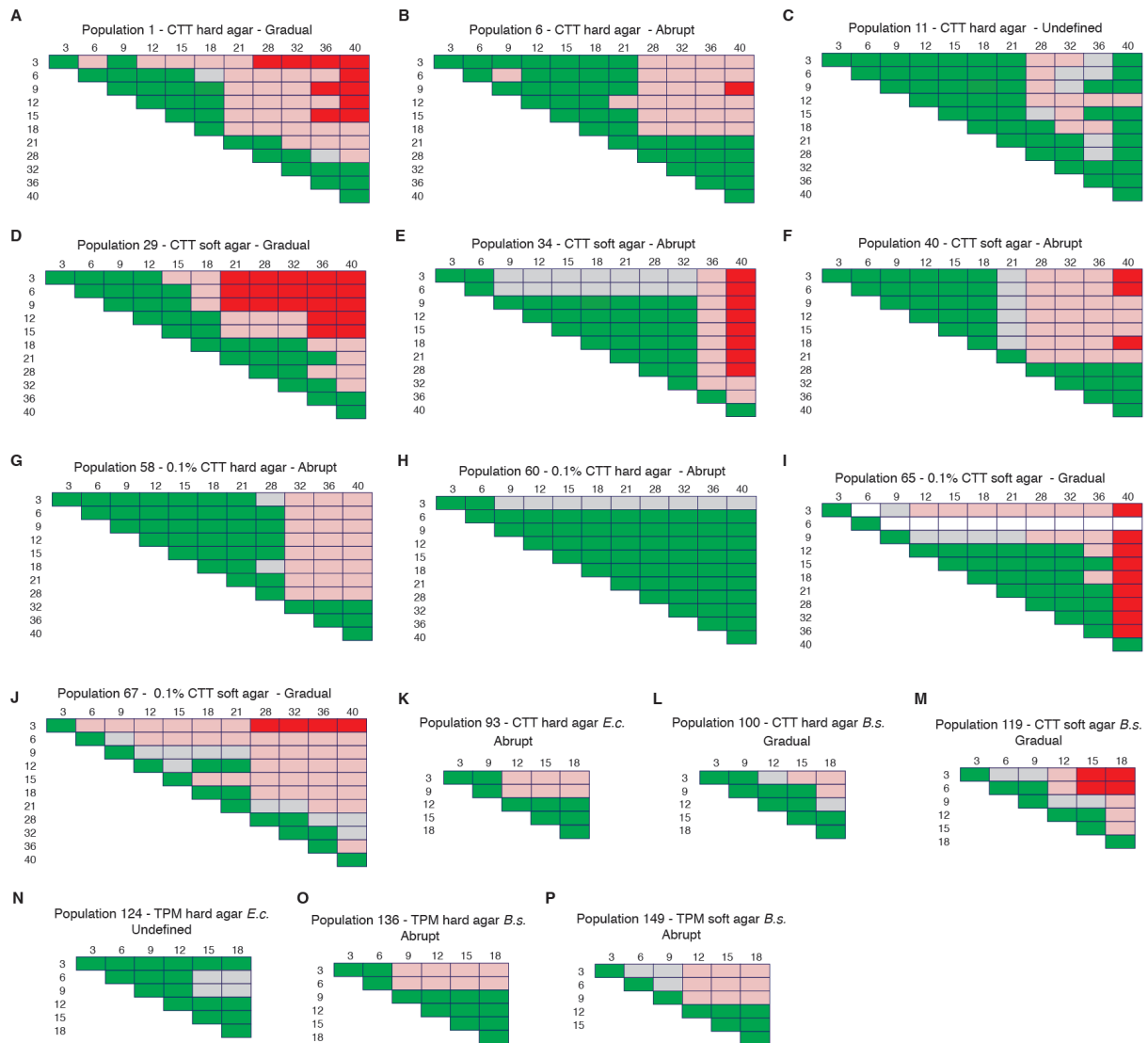


Figure S3. Kin discrimination patterns between temporal samples from the same population (KD-T). Colony-encounter phenotypes were examined between time-point samples from within the same population. Colors represent classifications described in Fig. 4. Axis numbers represent evolutionary time in selection cycles. Data for P10 and P35 are not shown but are included in Fig. 5. “Gradual” indicates that the probability of incompatibility is largely a function of evolutionary time whereas “abrupt” indicates a relatively discrete transition between compatibility states. “*E.c.*” indicates *E. coli* and “*B.s.*” indicates *B. subtilis*.

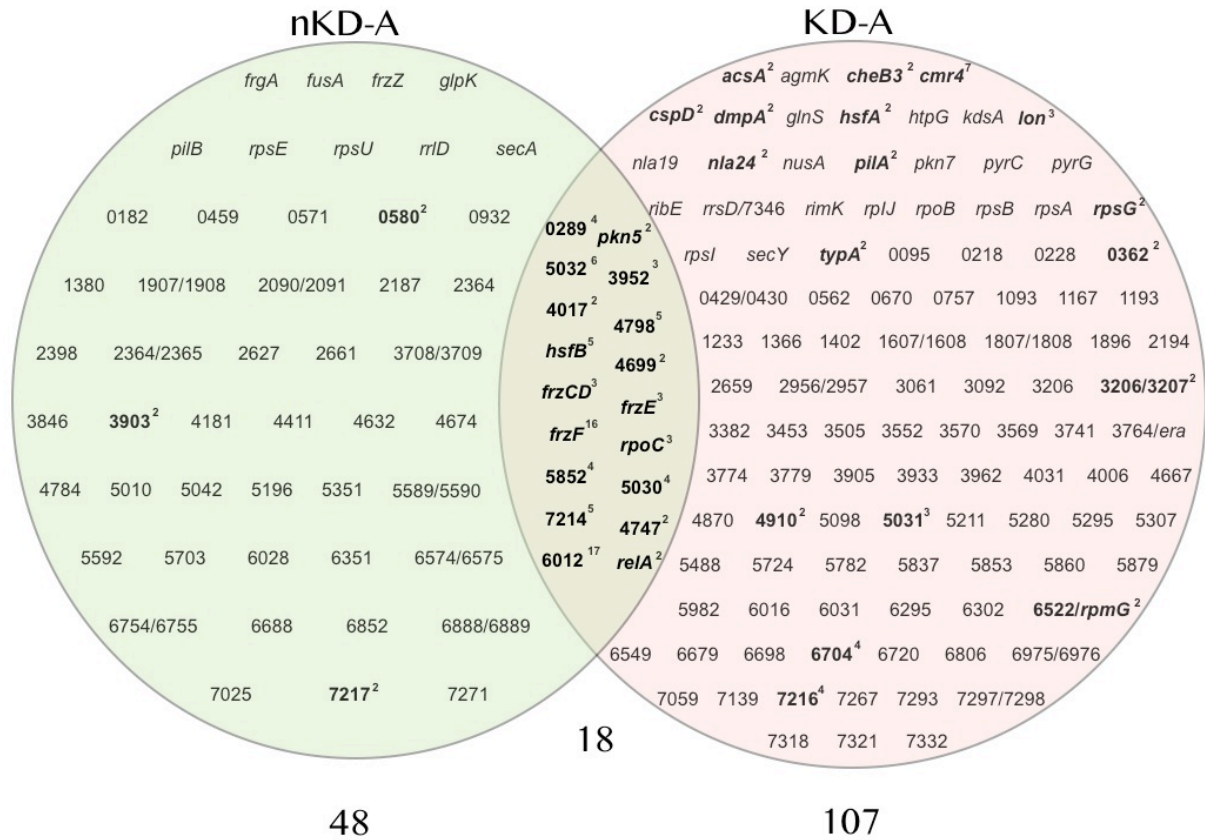


Figure S4. Venn diagram summarizing all mutated loci in clones from 23 evolved populations. Mutations analyzed from genome sequences of clones from 23 populations (excluding the clone from P29), sixteen of which displayed KD towards the ancestor (KD-A) and seven of which did not (nKD-A). Superscripts indicate the number of independently evolved populations that accumulated a mutation at the specified locus (i.e. instances of convergent evolution), whereas loci without superscripts depict singleton mutations unique to one population. A total of 173 independent mutations are represented, the majority of which (134) occurred in loci that were mutated in only one population (45 for nKD-A populations and 89 for KD populations). Eighteen loci were mutated in clones from both KD-A and nKD-A populations. Loci are identified either by their published gene names or respective “*MXAN*” locus tag number in case of uncharacterized loci.

SUPPLEMENTARY TABLES

Table S1. Fitness effects of forced mixing at a 1:1 ratio for two pairs of antagonistic natural isolates during multicellular development.

Paired two-tailed *t* tests were performed to compare appropriate parameters. N_i , total spores produced in pure culture (\log_{10}) per 5×10^8 initial cells; $N_i(j)$, spores produced by *i* in forced mixture with *j* per 5×10^8 initial cells; W_{ij}^* : \log_{10} -difference in pure-culture spore production of strains *i* and *j*; W_{ij} , relative fitness, or the observed difference in (\log_{10}) spore production of strains *i* and *j* during forced mixing. Values presented are the average of at least three independent replicates and corresponding upper and lower bounds of the 95% confidence intervals.

Forced Mix	Clone	N_i	W_{ij}^*	$N_i(j)$	W_{ij}	N_i vs. $N_i(j)$	W_{ij}^* vs. W_{ij}
A47 vs. A23	A47	7.91 ± 0.36	0.42 ± 0.34	7.45 ± 0.43	3.42 ± 1.38	$p = 0.064$	$p = 0.015$
	A23	7.49 ± 0.42	-0.42 ± 0.34	4.02 ± 1.48	-3.42 ± 1.38	$p = 0.009$	
A47 vs. A96	A47	7.75 ± 0.19	0.21 ± 0.23	6.85 ± 0.12	2.19 ± 0.85	$p = 0.043$	$p = 0.032$
	A96	7.71 ± 0.36	-0.21 ± 0.23	4.66 ± 0.74	-2.19 ± 0.85	$p = 0.009$	

Table S2. Experimental evolution treatments, populations and patterns of KD-A evolution. Odd-numbered populations descend from the rifampicin-sensitive ancestor GJV1 and the even-numbered populations descend from the rifampicin-resistant ancestor GJV2. **Bold blue text** indicates terminal populations that evolved a **clear and consistent KD-A phenotype** (55 populations), *italicized black text* indicates *inconsistent KD-A phenotypes* (seven populations) and standard black text indicates the absence of a KD-A phenotype (26 populations). *Asterisks indicate ancestral sub-clones found to have a shared mutation in *cmr4* (*cmr4*-P72H, see main text and Supplemental Results).

Treatment	Description	Cycles	Examined populations (organized by ancestral GJV1 or GJV2 sub-clone)												
			GJV 1.1*	GJV 2.1	GJV 1.2	GJV 2.2	GJV 1.3*	GJV 2.3	GJV 1.4	GJV 2.4	GJV 1.5*	GJV 2.5	GJV 1.6*	GJV 2.6	
CTT hard agar (HA)	1% Casitone, 1.5% agar	40	P1	P2	P3	P4	P5	P6	P7	P8	P9	P10	P11	P12	
CTT soft agar (SA)	1% Casitone, 0.5% agar	40	P29	P30	<i>P31</i>	<i>P32</i>	P33	P34	P35	P36	P37	P38	P39	P40	
Low nutrient CTT HA	0.1% Casitone, 1.5% agar	40	P57	P58	P59	P60	P61	<i>P62</i>	P63	P64					
Low nutrient CTT SA	0.1% Casitone, 0.5% agar	40	P65	P66	P67	P68									
CTT HA <i>E. coli</i>	<i>E. coli</i> grown on CTT HA	40	P89	P90	P91	P92	P93	P94	P95	P96					
CTT HA <i>B. subtilis</i>	<i>B. subtilis</i> grown on CTT HA	40	P97	P98		P100		P102	P103	P104					
CTT SA <i>E. coli</i>	<i>E. coli</i> grown on CTT SA	40	P105	P106	P107	P108		P110		P112					
CTT SA <i>B. subtilis</i>	<i>B. subtilis</i> grown on CTT SA	40	P113		P115	P116	P117	P118	P119						
TPM HA <i>E. coli</i>	<i>E. coli</i> overlaid on TPM HA	18	P121	P122	P123	P124	P125	<i>P126</i>	P127	<i>P128</i>					
TPM HA <i>B. subtilis</i>	<i>B. subtilis</i> overlaid on TPM HA	18	P129	P130	P131	P132	P133	P134	P135	P136					
TPM SA <i>E. coli</i>	<i>E. coli</i> overlaid on TPM SA	18	P137	P138		P140		<i>P142</i>		<i>P144</i>					
TPM SA <i>B. subtilis</i>	<i>B. subtilis</i> overlaid on TPM SA	18	P145	P146		P148	P149		P151						

Table S3. Kin discrimination between independent replicate populations from the same evolutionary treatment (KD-B).

Treatment	Examined pairs (<i>N</i>)	KD-B	% KD-B
CTT HA	28	15	54
CTT SA	22	15	69
0.1% CTT HA	12	7	59
0.1% CTT SA	3	2	67
CTT HA <i>E. coli</i>	8	4	50
CTT HA <i>B. subtilis</i>	6	3	50
CTT SA <i>E. coli</i>	6	6	100
CTT SA <i>B. subtilis</i>	10	3	30
TPM HA <i>E. coli</i>	10	2	20
TPM HA <i>B. subtilis</i>	1	1	100
TPM SA <i>E. coli</i>	7	1	15
TPM SA <i>B. subtilis</i>	4	3	75
Total	117	62	53

Table S4. Numbers of mutations accumulated in evolved clones after 40 two-week cycles. The genomes of single clones from each of 24 distinct populations were sequenced and the number of mutations in total and in four categories are shown.

<u>Population</u>	<u>KD-A phenotype</u>	<u>Evolutionary treatment</u>	<u>Total # of mutations</u>	<u>Genic</u>	<u>Coding</u>	<u>Synonymous</u>	<u>Intergenic</u>
P1	+	CTT HA	13	12	11	1	1
P2	-	CTT HA	13	10	8	2	3
P3	+	CTT HA	10	10	10	0	0
P4	-	CTT HA	10	9	9	0	1
P5	-	CTT HA	14	13	11	2	1
P6	+	CTT HA	12	11	10	1	1
P7	+	CTT HA	7	6	5	1	1
P8	+	CTT HA	9	9	8	1	0
P9	+	CTT HA	10	10	9	1	0
P10	+	CTT HA	10	10	7	3	0
P11	+	CTT HA	13	11	10	1	2
P12	-	CTT HA	19	15	14	1	4
P29	+	CTT SA	435	373	ND	ND	62
P30	+	CTT SA	13	13	10	3	0
P31	Undefined	CTT SA	16	15	12	3	1
P32	Undefined	CTT SA	12	12	11	1	0
P33	+	CTT SA	11	10	9	1	1
P34	+	CTT SA	13	13	11	2	0
P35	+	CTT SA	23	21	19	2	2
P36	+	CTT SA	14	14	13	1	0
P37	+	CTT SA	16	14	13	1	2
P38	-	CTT SA	10	10	9	1	0
P39	+	CTT SA	17	15	13	2	2
P40	+	CTT SA	13	12	11	1	1

Table S5. Genes mutated in more than two populations. Seventeen of the sequenced clones from 24 populations exhibited clear and consistent KD-A (71%) and seven did not. The third through sixth columns show the number of populations mutated at the respective locus, the number and percentage of those populations that show a KD-A phenotype and the number of distinct mutation sites, respectively.

Mutated locus	Description	No. mutated clones	No. in KD-A clones	% KD-A	No. distinct mutations	Mutated populations
<i>MXAN_6012</i>	response regulator	17	11	65	10	P1, P2, P3, P5, P7, P8, P12, P30, P31, P32, P33, P34, P35, P36, P38, P39, P40
<i>frzF</i>	protein methyltransferase FrzF	17	13	76	13	P1, P3, P5, P8, P9, P10, P11, P29, P30, P31, P32, P33, P35, P37, P38, P39, P40
<i>MXAN_5852</i>	sensory box histidine kinase	9	5	56	6	P5, P30, P31, P32, P33, P35, P36, P37, P38
<i>cmr4</i>	CRISPR-associated RAMP protein Cmr4	8	8	100	1	P1, P7, P9, P11, P29, P35, P37, P39
<i>MXAN_5032</i>	efflux transporter, HAE1 family, inner membrane component	6	4	67	6	P5, P34, P35, P36, P37, P38
<i>MXAN_4798</i>	hypothetical protein	5	3	60	4	P10, P30, P31, P32, P36
<i>hsfB</i>	response regulator/sensor histidine kinase HsfB	5	3	60	5	P1, P5, P9, P12, P36
<i>MXAN_7214</i>	RNA polymerase sigma-70 factor, ECF subfamily	5	2	40	5	P1, P2, P6, P32, P38
<i>MXAN_7216</i>	ICE-like protease (caspase) p20 domain protein	4	4	100	4	P3, P7, P9, P11
<i>MXAN_5030</i>	efflux transporter, HAE1 family, outer membrane efflux protein	4	2	50	3	P31, P32, P33, P40
<i>MXAN_0289</i>	putative membrane protein	4	2	50	4	P3, P5, P12, P40
<i>MXAN_6704</i>	acetyltransferase, GNAT family	4	4	100	4	P6, P30, P34, P39
<i>lon</i>	ATP-dependent protease La	4	4	100	5	P29, P33, P35, P37
<i>frzCD</i>	frizzy aggregation protein FrzCD	4	2	50	4	P2, P7, P12, P29
<i>rpoC</i>	DNA-directed RNA polymerase subunit beta	3	2	67	3	P32, P34, P35
<i>MXAN_5031</i>	HAE1 family efflux transporter MFP subunit	3	3	100	3	P9, P30, P39
<i>frzE</i>	gliding motility regulatory protein	3	2	67	3	P6, P12, P36
<i>MXAN_3952</i>	sigma-54 dependent transcriptional regulator, Fis family	3	1	33	1	P4, P12, P37

Table S6. Mutations that first appeared in three independently evolved populations at the same transfer cycle that KD towards the ancestor (KD-A) first appeared.

Population	Gene	Function
P10	<i>MXAN_1574</i>	TfoX domain protein
	<i>MXAN_4006</i>	peptidase, S1C (protease Do) subfamily
	<i>agmK</i>	adventurous gliding motility protein AgmK
	<i>MXAN_5837</i>	bacterial Ig-like domain (group 1)/fibronectin type III domain protein
P33	<i>MXAN_5852</i>	sensory box histidine kinase
	<i>lon</i>	ATP-dependent protease La
P34	<i>rpsB</i>	ribosomal protein S2
	<i>MXAN_6704</i>	acetyltransferase, GNAT family

METHODS

Semantics. We adopt a broad definition of kin discrimination, namely any ‘alteration of social behavior as a function of genetic relatedness among interactants’. This definition is merely phenomenological and is thus entirely decoupled from the evolutionary, behavioral and molecular causes of kin discrimination traits, whatever those may be. Such causes must be determined independently of the mere demonstration that kin discrimination, as defined here, occurs in any given biological system. Thus, the definition encompasses both social adaptations *per se* and indirect byproducts of non-adaptive processes (or alternative adaptive processes) at the level of evolutionary causation, as well as organismal behaviors and molecular mechanisms of all degrees of complexity.

We define ‘colony-merger incompatibility’ as a reduced degree of merger by oncoming colonies each composed of a distinct genotype into one social group, relative to oncoming colonies that are composed of the same genotype. Colony-merger incompatibilities are phenotypically variable rather than a single discrete phenomenon, and can result in phenotypes ranging from a complete absence of contact between the cells at the leading edge of colony expansion to a slight but detectable reduction in the degree of colony inter-penetration relative to controls.

Strains, experimental evolution and growth conditions.

(i) *Experimental evolution.* Parallel evolving populations were initiated from independently isolated sub-clones of the two ancestral strains GJV1 (1), a rifampicin-sensitive clonal derivative of DK1622 (2) and GJV2, a rifampicin-resistant clonal derivative of GJV1. Six sub-clones each of GJV1 and GJV2 (GJV1.1 – GJV1.6 and GJV2.1 – GJV2.6) were stored frozen. All twelve sub-clones were used to initiate evolutionary the CTT hard and soft agar treatments (populations P1 - P12 and P29 - P40) whereas GJV1.1 – GJV1.4 and

GJV2.1 – GJV2.4 were used to initiate all other treatments (Table S2). Odd and even numbered populations derived from GJV1 and GJV2 sub-clones, respectively. The numerical order of population designators corresponds with the numerical order of sub-clone designators. For example, sub-clones GJV1.1, GJV2.1, GJV1.2, GJV2.2, GJV1.3, GJV2.3, etc. founded populations P1, P2, P3, P4, P5, P6, etc.; P29, P30, P31, P32, P33, P34, etc. and so on (Table S2).

All evolving populations were initiated and propagated as described previously (3) (see Fig. S2 and Table S2 for summary). Briefly, culture samples from ancestral clones ($\sim 5 \times 10^7$ cells in 10 μ l) were placed in the center of agar plates (InvitrogenTM Select Agar) and allowed to grow and swarm outward for two weeks at 32 °C and 90% rH. After two weeks, a sample of ~ 3 mm x 5 mm (~ 15 mm²) from the leading edge of each swarming colony was harvested with a sterile scalpel and transferred upside down at the center of a new plate. If a colony was not circular at the time of transfer, the sample was taken from the point along the colony edge farthest from the center. This transfer protocol was repeated every two weeks for either 18 or 40 cycles. Evolution experiments were carried out at the Max-Planck Institute for Developmental Biology in Tübingen, Germany from 2001-2003. All post-evolution assays were performed at ETH Zürich from 2012-2014 in at least three temporally independent replicates.

(ii) *Evolution environments.* Experimental evolution was performed in twelve distinct laboratory environments with either eight or twelve replicate populations each. Environments varied in nutrient source (bacterial prey vs. media substrate), nutrient level, surface viscosity (thus affecting motility evolution) and other parameters (Table S2).

Non-prey treatments: One day prior to colony transfer, 50 ml of either CTT (8 mM MgSO₄, 10 mM Tris pH 8.0, 10 g/L Casitone, 1 mM KPO₄) or 0.1% Casitone CTT (identical to CTT except with only 1 g/L Casitone) agar (hard or soft: 1.5% or 0.5% agar, respectively)

were poured into 14 cm-diameter petri dishes. Plates were allowed to solidify uncovered in a laminar flow hood (for 15-20 minutes) and then stored overnight at room temperature.

Prey treatments: Two days prior to transfer, agar plates were poured as previously described, including with TPM buffer, which is identical to CTT medium except without any Casitone. The next day, prey (*Bacillus subtilis* PY79 (4) or *Escherichia coli* REL607 (5)) were inoculated into three flasks containing 900 ml of CTT liquid and grown overnight at 32 °C, 300 rpm. On the transfer day, 200 µL of grown prey were spread out on CTT plates for CTT + prey environments. For TPM + prey plates, prey cultures were centrifuged in 500 mL tubes at 4 °C, 10,000 rpm for 10 minutes. The supernatant was discarded and pellets were resuspended in 3 mL of TPM by shaking at 400 rpm. Resuspended pellets of each prey type were pooled and 1 mL of prey suspension was spread out over the entire surface of TPM plates and allowed to dry. Cycles transfers were then performed as described above. Plates were kept upright for one night and then turned upside down. (iii) *Growth conditions*. All evolution and post-evolution agar-plate cultures were incubated at 32 °C, 90% rH. For post-evolution experiments, cultures initiated from frozen stocks were grown on CTT hard agar plates for three or four days. Prior to the start of each experiment, culture samples were transferred from plates to 8 mL CTT liquid (in 50 mL flasks) for 24 hours at 32°C with constant shaking at 300 rpm until they reached mid exponential phase ($OD_{600} = \sim 0.5$).

Colony-encounter assays. (Some text in this section is replicated from **Methods** for clarity.)

To assess whether evolved populations discriminate between themselves and their ancestor (KD-A), samples from other evolutionary time-points from the same population (KD-T) or other evolved populations from the same evolutionary environment (KD-B), we staged colony-encounter assays as follows. One day prior to each assay, cells were inoculated in liquid media and plates were prepared by pouring 20 mL CTT soft agar (0.5% agar) into 9

cm-diameter petri dishes unless otherwise specified. Plates were allowed to solidify uncovered in a laminar flow hood (for 15-20 minutes) and stored overnight at room temperature. To start each assay, 10 μL of each culture (previously adjusted to $\sim 5 \times 10^9$ cells/mL) were spotted 1 cm apart from each other. In experimental assays testing for KD-A (see main text), one spot on a plate contained the ancestor and the other contained an evolved population. In experimental assays testing for between-population KD-B or KD-T, the two spots on a plate were from distinct evolved populations or different evolutionary time-points within the same population, respectively. In control assays, two spots of the same genotype (or population sample) were tested for colony merger. Such self-self encounter controls were performed for all assayed strains and populations simultaneously with experimental treatments. After spotting, culture samples were allowed to dry in a laminar flow hood and plates were then incubated for three days, after which colonies were examined for the presence or absence of a clearly discernable line of demarcation between swarms. Colony-interface phenotypes were photographed and classified into four qualitative categories: a) freely merging (no visually detectable difference from self-self encounter controls of the ancestor, green in Figs. 4, 5 and S3), b) consistently reduced merger of intermediate phenotypic strength (light red), c) consistently and greatly reduced merger or complete non-merger (red), and iv) inconsistent phenotypes across replicate experiments (grey). Such inconsistencies may have been due to differential behavior of genetically heterogeneous populations across experimental replicates. The small minority of pairings that yielded highly inconsistent results was excluded from statistical analysis. Colony pairings not performed, or not analyzed due to contamination events are represented by white matrix cells in Figs. 4 and S3.

Fruiting body chimerism assays.

To test whether colony-merger incompatibilities reduce developmental co-aggregation of distinct genotypes along fruiting bodies near the inter-colony borders, we assessed the frequency of chimerism across fruiting bodies. Cultures were prepared as described above. A day prior to the assay, plates were prepared by pouring 9 mL of CF agar (a low-nutrient medium that allows some growth and swarming before development is initiated upon nutrient depletion; ref. 6; 10 mM Tris pH 8.0, 1 mM KH₂PO₄, 8 mM MgSO₄, 0.02% (NH₄)₂SO₄, 0.2% citrate, 0.1% pyruvate, 150 mg/L Casitone) into 5 cm-diameter petri dishes. Ten microliters of each culture adjusted to $\sim 5 \times 10^9$ cells/mL were spotted one centimeter apart from each other, allowed to dry in a laminar flow hood and incubated at 32 °C, 90% rH. After six days, four to eight individual fruiting bodies adjacent to the interface of oncoming swarms were harvested and their respective locations relative to the interface documented for each. Individual fruiting bodies were incubated in 500 μ L sterile ddH₂O at 50 °C for two hours to select for viable, heat-resistant spores. Samples were sonicated with a sterile microtip, diluted in sterile ddH₂O and plated in CTT soft (0.5%) agar containing the appropriate antibiotics. All mixes were performed at least three times in temporally independent blocks. Experimental treatments and controls were performed simultaneously with each mixed culture assay. *M. xanthus* natural clones A23, A47 and A96 were isolated from a 16 x 16 cm soil plot in Tübingen, Germany as described previously (7). Rifampicin- and kanamycin-resistant variants of natural isolates (specified by ‘R’ and ‘K’, respectively, in Figs. 1 and S1) were previously characterized (8) and had no significant defects in pure culture spore production.

Whole-genome sequencing and mutation identification.

Genomic DNA (>30 µg) was extracted from exponentially growing cells using Qiagen's Genomic DNA Isolation Kit and 100G Genomic-Tip. Illumina HiSeq sequencing was performed by BGI Tech Solutions Co., Ltd. (Hong Kong, China) and yielded a total of ~10⁹ bp of sequence per genome, or ~100-fold average coverage. Small genomic changes were identified for each genome by mapping reads against the reference genome of *M. xanthus* DK1622 (NC_008095.1) using *breseq v0.21* (9). Five known SNPs between the DK1622 derivative used as the ancestor in these studies (GJV1 (1)) and the published sequence of DK1622 (2) as well as a known *rpoB* mutation in GJV2-derived (rifampicin-resistant) populations served as positive controls for the reliability of mutation identification. All five polymorphisms shared by all evolved clones were detected in all 24 sequenced genomes and the *rpoB* mutation was detected in all twelve of the rifampicin-resistant clones. Additionally, a subset of polymorphisms in evolved clones was checked by sequencing PCR products.

SUPPLEMENTARY RESULTS

While several genes evolved convergently (at the gene level) among the 24 genome-sequenced clones, only one locus, the CRISPR-associated gene *cmr4*, was mutated exclusively in KD-A populations (Tables S2 and S5). CRISPR genes protect bacterial cells against mobile genetic elements such as viruses and plasmids and also regulate social traits such as virulence and biofilm formation in *Campylobacter jejuni* and *Pseudomonas aeruginosa*, respectively, as well as multicellular development in *M. xanthus* (10, 11). Surprisingly, the same nonsynonymous mutation in *cmr4* (amino acid substitution P72H) was found in all populations mutated at this locus, whereas for all other loci that were mutated in four or more populations, the precise mutations in those genes differed across most

populations (Table S5). This pattern suggested that the *cmr4* mutation might be causally related to the evolution of kin discrimination in at least some populations.

To investigate this possibility further, all populations were tested for *cmr4* mutations at their terminal time point. The *cmr4* mutation P72H was found in approximately one third of all populations, but during the process of tracing the temporal origins of this mutation we noted that it was only present in populations derived from four specific ancestral sub-clones and not in populations derived from the other eight sub-clones. We thus hypothesized and subsequently confirmed that this mutation was present in four sub-clone ancestors used to initiate experimental populations (GJV1.1, GJV1.4, GJV1.5 and GJV1.6, see Table S2), but was not present in GJV1.2, GJV1.3 or in any of the six GJV2 sub-clones. This finding implies that the source culture of GJV1 used to isolate the GJV1.1-1.6 sub-clones was polymorphic for this mutation prior to sub-clone selection and the onset of experimental evolution.

Our tracing of the *cmr4*-P72H mutation to a subset of ancestral sub-clones is of interest for both methodological and evolutionary reasons. Methodologically, for microbial experimental evolution studies this finding highlights the importance of initiating replicate populations of a clonal ancestral strain from independently isolated sub-clones of that strain that are themselves stored frozen for future reference. Given that all microbial cultures larger than a few thousand individuals are expected to be polymorphic due to spontaneous mutation (12), curation of ancestral sub-clones allows determination of whether identical mutations found in distinct replicate populations evolved convergently or not.

Evolutionarily, among the 55 populations that evolved clear and consistent KD-A phenotypes, the proportion that derived from a sub-clone ancestor that carried the *cmr4*-P72H mutation (20/55, 36%) is improbable under the null hypothesis that the ancestral presence of this mutation and the probability of evolving KD-A are causally unrelated, relative to the

much lower frequency of ancestral *cmr4*-P72H carriage among the remaining populations (4/29, 14%; two-tailed $p = 0.042$, Fisher's exact test). This outcome suggests the hypothesis that carriage of *cmr4*-P72H causally increases the probability of evolving of KD-A relative the absence of this mutation (even though KD-A did evolve in many populations not carrying this mutation).

A second evolutionary pattern is also statistically associated with the ancestral presence of *cmr4*-P72H. Among the 18 populations for which KD-T phenotype patterns were analyzed temporally, seven exhibited relatively gradual KD-T emergence patterns whereas nine showed abrupt KD-T appearance and two showed an intermediate pattern (Fig. 4 and Figs. S2 and S3). Of these 18 populations, all six that carried the ancestral *cmr4* mutation (P1, P29, P35, P65 and P119) exhibited gradual KD-T emergence, an outcome with very low probability under the null expectation that carriage of *cmr4*-P72H does not affect the temporal pattern of KD evolution (two-tailed $p = 0.0009$, Fisher's exact test with the two intermediate-pattern populations excluded). The absence of *cmr4*-P72H in one gradual-KD-T population shows that this pattern can evolve without the mutation, but the overall distribution of KD-T evolution patterns suggests that carriage of *cmr4*-P72H may promote the gradual evolution of KD-T rather than its abrupt appearance.

REFERENCES

1. Velicer GJ, *et al.* (2006) Comprehensive mutation identification in an evolved bacterial cooperator and its cheating ancestor *Proc Natl Acad Sci USA* 103(21): 8107–8112.
2. Goldman BS, *et al.* (2006) Evolution of sensory complexity recorded in a myxobacterial genome. *Proc Natl Acad Sci USA* 103(41):15200-15205.
3. Velicer GJ & Yu YT (2003) Evolution of novel cooperative swarming in the bacterium *Myxococcus xanthus*. *Nature* 425(6953):75-78.
4. Youngman P, Perkins JB, & Losick R (1984) Construction of a cloning site near one end of Tn917 into which foreign DNA may be inserted without affecting transposition in *Bacillus subtilis* or expression of the transposon-borne Erm gene. *Plasmid* 12(1):1-9.
5. Lenski RE, Rose MR, Simpson SC, & Tadler SC (1991) Long-term experimental evolution in *Escherichia coli*. I. Adaptation and divergence during 2,000 generations. *Am Nat* 138(6):1315-1341.
6. Hagen DC, Bretscher AP, & Kaiser D (1978) Synergism between morphogenetic mutants of *Myxococcus xanthus*. *Dev Biol* 64(2):284-296.
7. Vos M & Velicer GJ (2006) Genetic population structure of the soil bacterium *Myxococcus xanthus* at the centimeter scale. *Appl Environ Microbiol* 72(5):3615-3625.
8. Vos M & Velicer GJ (2009) Social conflict in centimeter-and global-scale populations of the bacterium *Myxococcus xanthus*. *Curr Biol* 19(20):1763-1767.
9. Deatherage DE & Barrick JE (2014) Identification of mutations in laboratory-evolved microbes from next-generation sequencing data using breseq. *Methods Mol Biol* 1151:165-188.
10. Viswanathan P, Murphy K, Julien B, Garza AG, & Kroos L (2007) Regulation of *dev*, an operon that includes genes essential for *Myxococcus xanthus* development and CRISPR-associated genes and repeats. *J Bacteriol* 189(10):3738-3750.
11. Westra ER, Buckling A, & Fineran PC (2014) CRISPR-Cas systems: beyond adaptive immunity. *Nature Rev Microbiol* 12(5):317-326.
12. Bromham L (2009) Why do species vary in their rate of molecular evolution? *Biol Letters* 5(3):401-404.